J|A|C|S
COMMUNICATIONS

Published on Web 06/03/2004

Effect of Halo Substitution on the Geometry of Arenethiol Films on Cu(111)

Kin Wong, Ki-Young Kwon, Bommisetty V. Rao, Anwei Liu, and Ludwig Bartels*

Pierce Hall, University of California−Riverside, Riverside, California, 92521

Received March 9, 2004; E-mail: ludwig.bartels@ucr.edu

Thiol films on noble metal surfaces attract considerable interest due to their ability of facile self-assembly from the solution phase.[1] Films of only monomolecular thickness can modify the electronic, physical, and chemical properties of the underlying substrate dramatically. This offers powerful opportunities for fundamental studies of electron transport,[2] single-molecule devices (e.g., tunneling diodes[3] or transistor[4]), control of surface wettability,[5] etc. The formation of thiol films is driven predominantly by strong substrate−sulfur interactions. At saturation coverage, the result is a layer of molecules that stand close to upright on the surface. For alkanethiols on Au(111), $(\sqrt{3} \times \sqrt{3})R30°$ and related superlattices were inferred.[6−8] In a solution environment, it is difficult to follow the initial stages of thiol chemisorption because of their high surface mobility prior to formation of a dense film and the presence of the surrounding solution. Vacuum deposition of thiols allows the study of low coverages, and a large variety of different alkanethiols patterns have been reported.[9−12] To the best knowledge of the authors, low coverages of arenethiols have not been addressed so far, although arenethiols have much larger potential for electronic applications than alkanethiols. This study uses thiophenol (TP) and its *p*-bromo- (BTP), *p*-chloro- (CTP), *p*-fluoro- (FTP), and pentafluoro-substituted (5FTP) analogues as model compounds for arenethiol film formation and explores the impact of a slight variation of arenethiol size and substituent electronegativity (EN) on the films' structural properties. We studied a broad range of coverages and found the most dramatic effects at incomplete films, where the molecules aggregate into isolated islands that are separated by empty terraces.

We used two home-built STM systems that were operated in UHV ($<10^{-10}$ Torr) at cryogenic temperatures (15 or 81 K). Multiple cryopanels enclosed the STMs in order to minimize drift and sample contamination. We used a Cu(111) single crystal as a substrate. Sample preparation involved cycles of sputtering (Ar, 1.5 keV) and annealing (600 K). All arenethiol coverages were prepared by backfilling the chamber to a pressure of $\sim 10^{-9}$ Torr and (if necessary, multiple cycles of) sample exposure for ~15 s.

We observed spontaneous formation of the superlattices in Figure 1 at 81K, which suggests that they may form transiently during the deposition of larger coverages.

Figure 1a,b shows STM images of isolated CTP and TP molecules at 15 K after hydrogen abstraction. The molecules adsorb flat on the surface, and their image has a depression that we associate with the position of the thiol group. Using lateral manipulation[13] and coadsorption of CO for registry,[14] we find that both the S and the halogen atoms occupy Cu(111) hollow sites. The overall shape of FTP, 5FTP, and BTP is similar to Figure 1a,b and their size scales with the dimension of the substituent(s). Figure 1c−f shows a clean Cu(111) surface and islands of the para-substituted molecules. Fourier transformation (FT) of the structures represents their periodicity at high fidelity. A FT is similar to a LEED pattern taken on a *single-domain* film, but it avoids film degradation common with conventional LEED systems.[15] The Cu(111) step height is used as an internal calibration standard, which allows direct comparison between the film structure at 81 K and the Cu(111) periodicity at 15 K.

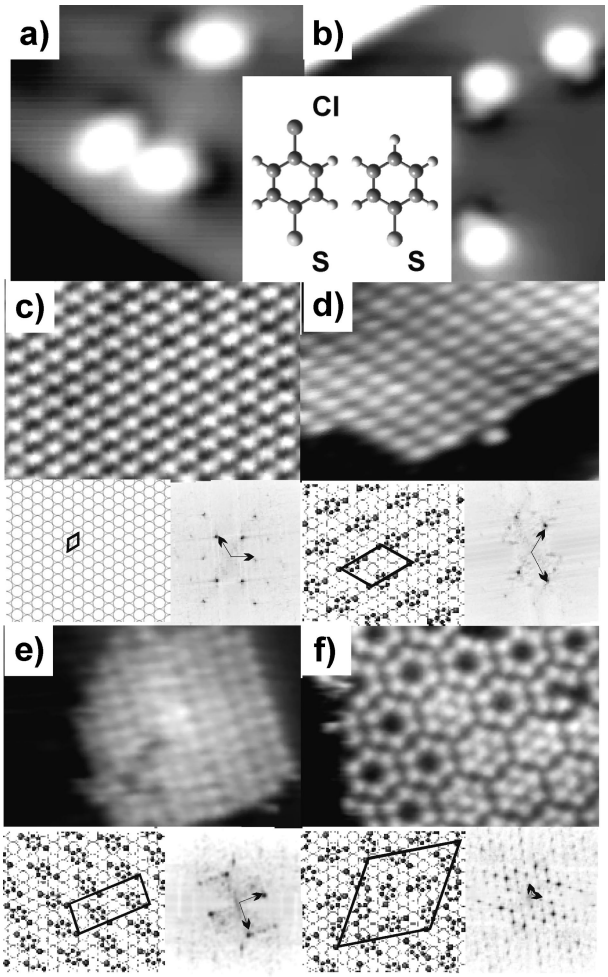

Figure 1. (a,b) STM images of CTP and TP molecules adsorbed on Cu(111). The sulfur anchors appear as depressions (32/51 pA, −300/−350 mV, 43 × 43 Å, 15 K). (c−f) STM images, models and FTs (computed from extended areas of the same structure) of (c) clean Cu(111) (51 pA, 250 mV, 33 × 22 Å, 15 K), (d) BTP/Cu(111) (47 pA, 1.2 V, 110 × 76 Å, 81 K), (e) CTP/Cu(111) (30 pA, 0.58 V, 110 × 76 Å, 81 K), (f) FTP/Cu(111) (31 pA, 1.7 V, 110 × 76 Å, 81 K). The indicated reciprocal lattice vectors are as follows (theoretical values in parentheses): (c) 2.87, 2.80 $Å^{-1}$ (both 2.84 $Å^{-1}$); (d) 0.98, 0.75 $Å^{-1}$ (0.95, 0.71 $Å^{-1}$); (e) 0.95, 0.75 $Å^{-1}$ (0.93, 0.75/2 $Å^{-1}$); (f) 0.37, 0.34 $Å^{-1}$ (both 0.36 $Å^{-1}$).

Careful analysis of Figure 1d,f allows us to deduce the periodicity inside the island: BTP exhibits a (4 × 3) pattern, which corresponds to a coverage of 1 BTP per 12 Cu atoms, i.e., 0.083 ML. In the (4 × 3) structure, all molecules are aligned in parallel and the Br and S atoms of neighboring molecules face each other.

Substitution of Br with Cl decreases the footprint of the molecule slightly, which results in a $\begin{bmatrix} 7 & -1 \\ -1 & 3 \end{bmatrix}$ pattern with two molecules in the unit cell. In this pattern, the thiol anchors of adjacent

10.1021/ja048660h CCC: $27.50

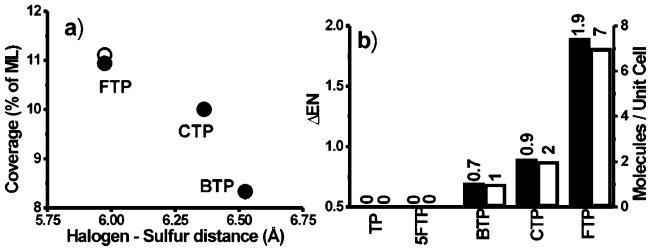

Figure 2. (a) Molecular density in the islands versus S−X distance (open circle = (3 × 3) pattern). The error bars are smaller than the dots (i.e., 0.001 ML). (b) Correspondence between the number of molecules per unit cell (as an indicator of the superlattice complexity) and EN difference (as an indicator of QM).

molecules reside in different hollow sites (hcp vs fcc). Consequently, the surface pattern consists of rows of pairs of molecules, with adjacent rows of molecules (or pairs of molecules) offset by 1/2 adsites to avoid on-top placement of their sulfur anchors. The CTP molecules align almost in parallel, while S and Cl atoms of adjacent molecules are offset transversely from one another. The result is an almost rectangular pattern at a coverage of 1/10 = 0.100 ML.

In contrast to the relatively simple patterns of BTP and CTP, FTP forms a honeycomb structure composed of six-membered rings of molecules, whose S−F axes are oriented close to tangential. The center of the honeycomb frequently remains vacant (see Figure 1f), which indicates a slightly lower binding energy here. This structure has (8 × 8)R19° symmetry, and its density is only $<2 \times 10^{-3}$ ML smaller than that of a (3 × 3) structure (0.109 vs 0.111 ML). While we can find small patches of (3 × 3) upon deposition, annealing to ∼200 K confirms that the (8 × 8)R19° structure is indeed the thermodynamic equilibrium as long as free adsorption sites are available on the surface. We confirmed the theoretically expected difference in coverage to 10^{-4} ML by analyzing the position of ∼10 000 FTP molecules.

TP and 5FTP do not form ordered islands under our experimental conditions. In particular, we followed the diffusion of TP molecules over 1 month (>25 000 images) at various temperatures. This dataset shows the formation and diffusion of clusters of 1−7 TP molecules; however, no aggregation to ordered islands is observed. Similar results were obtained for 5FTP.

Finally, we explored the origin of the difference in island aggregation behavior between the arenethiols. Figure 2a shows that with increasing size of the arenethiols (as calculated from standard bond lengths[16]), the density of the corresponding superlattice decreases.

Much more surprising is the increase of the superlattice complexity in our dataset: while TP and 5FTP do not form any regular pattern at all, the complexity of the ordered patterns seems to increase from the relative simple arrays of BTP and CTP to the beautiful and intricate honeycomb of FTP. Although the relation between molecular size and substrate periodicity imposes some restrictions on the possible superlattice geometries, Figure 2a shows that this consideration cannot explain why FTP prefers the (8 × 8)R19° over the (3 × 3) lattice (open circle in Figure 2a).

Unfortunately, a rigorous ab initio calculation of the minimal energy superlattice appears to be impractical due to the large unit cell involved. Consequently, we restricted ourselves to a model that is based predominantly on the intrinsic properties of the arenethiols. In the gas phase, the dipole moments of FTP, CTP, and BTP are expected to fall between those of TP and 5FTP.[17] If we assume that substrate interactions will change the magnitude but not the sequence of the molecular dipole moments, then the absence of order in TP and 5FTP islands suggests that the dipolar character of the investigated arenethiols is insufficient for causing the observed patterns. Theoretical investigation of alkanethiols adsorption indicates that the substrate donates ∼1/2 e− charge to the sulfur atom.[18] With increasing EN of the para substituent (Br, 2.8; Cl, 3; F, 4), more and more charge is pulled to its side. If the substituents in meta/ortho position have a lower EN, then a strong molecular quadrupole moment (QM) results. Figure 2b shows $\Delta EN = EN_{para} - EN_{meta/ortho}$ for the investigated arenethiols. As an indicator of the superlattice complexity, we also plot the numbers of molecules per unit cell (assuming 0, if no ordered structure is found). The sharp rise of the superlattice unit cell size at increasing ΔEN leads us to propose that the observed superlattices geometries reflect quadrupolar intermolecular interactions.

Quadrupolar interactions correspond to repulsion between sulfur and halogen atoms of adjacent molecules and attraction between an S or X atom of one molecule and the aromatic ring of its neighbor. Consistently, we find that for BTP (low QM) the S and Br atoms face each other and approach neighboring aryl moieties only by an offset between adjacent molecular rows. The CTP superlattice (intermediate QM) shows a similar offset between adjacent rows. In addition, a transversal offset separates the S and Cl atoms. Finally, FTP (strong QM) forms circular patterns, in which both S and F atoms approach neighboring aryl rings as closely as possible. Only the center sites, which are often found to be empty, do not follow this trend strictly.

In conclusion, we analyzed the structure of isolated islands of various arenethiols on Cu(111) at cryogenic temperatures and found that the complexity of the patterns correlates with the intrinsic QM of the molecules. We note that if quadrupolar interactions, which are generally assumed to be weak, are capable of determining arenethiol film patterns, a careful choice/synthesis of specific substituents may present an avenue toward film patterns of almost arbitrary symmetry.

Acknowledgment. This work was supported by NSF (CHE-0132996, DMR-0116339), DOE (DE-FG03-03ER15464), AFOSR (F49620-01-1-0286), and PRF (36987-G5).

References

(1) Ulmann, A. *Self-Assembled Monolayer of Thiols*; Academic Press: New York, 1998.
(2) Xu, B.; Tao, N. J. *Science* **2003**, *301*, 1221−1223.
(3) Fan, F. R. F.; Yang, J. P.; Cai, L. T.; Price, D. W.; Dirk, S. M.; Kosynkin, D. V.; Yao, Y. X.; Rawlett, A. M.; Tour, J. M.; Bard, A. J. *J. Am. Chem. Soc.* 2002, *124*, 5550−5560.
(4) Park, J.; Pasupathy, A. N.; Goldsmith, J. I.; Chang, C.; Yaish, Y.; Petta, J. R.; Rinkoski, M.; Sethna, J. P.; Abruna, H. D.; McEuen, P. L.; Ralph, D. C. *Nature* **2002**, *417*, 722.
(5) Lahann, J.; Mitragotri, S.; Tran, T. N.; Kaido, H.; Sundaram, J.; Choi, I. S.; Hoffer, S.; Somorjai, G. A.; Langer, R. *Science* **2003**, *299*, 371−374.
(6) Noh, J.; Hara, M. *Langmuir* **2002**, *18*, 1953−1956.
(7) Poirier, G.; Tarlov, M. J. *Langmuir* **1994**, *10*, 2853.
(8) Delamarche, E.; Michel, B.; Gerber, C.; Anselmetti, D.; Guntherodt, H. J.; Wolf, H.; Ringsdorf, H. *Langmuir* **1994**, *10*, 2869.
(9) Driver, S. M.; Woodruff, D. P. *Langmuir* **2000**, *16*, 6693−6700.
(10) Poirier, G. E.; Pylant, E. D. *Science* **1996**, *272*, 1145−1148.
(11) Kühnle, A.; Vollmer, S.; Linderoth, T. R.; Witte, G.; Wöll, C.; Besenbacher, F. *Langmuir* **2002**, *18*, 5558−5565.
(12) Lee, J.-G.; Yates, J. T., Jr. *J. Phys. Chem. B* **2003**, *107*, 10540−10545.
(13) Bartels, L.; Rao B. V.; Liu, A. *Chem. Phys. Lett.* **2004**, *385*, 36.
(14) Rao, B. V.; Kwon, K.-Y.; Liu, A.; Bartels, L. *J. Chem. Phys.* **2003**, *119*, 10879−10884.
(15) Microchannel plate LEED avoids radiation damag, e.g.: Azzam, W.; Cyganik, P.; Witte, G.; Bucks, M.; Wöll, Ch. *Langmuir* **1999**, *19*, 8262.
(16) Kong J. et al. *J. Comput. Chem.* **2000**, *21*, 1532.
(17) We checked this by DFT calculation of isolated arenethiols as described in ref 16.
(18) Ferral A.; Paredes-Olivera P.; Macagno V. A.; Patrito, E. M. *Surf. Sci.* **2003**, *525*, 85−99.

JA048660H